

Research article

Investigating the effect of post-weld heat treatment on the corrosion properties of the explosive welded three-layer joint of Cu/Al/Cu

H. A. Zamani¹, M. R. Khanzadeh^{2*}, A. Bakhtiari³, H. Paydar⁴

¹ Masters, Department of Material Engineering, Islamic Azad University, Majlesi Branch, Esfahan, Iran.

² Associate Professor, Faculty of Engineering, Mobarakeh Branch, Islamic Azad University, Esfahan, Iran.

³ Assistant Professor, Department of Material Engineering, Islamic Azad University, Majlesi Branch, Esfahan, Iran

⁴ Assistant Professor, Center for Advanced Engineering Research, Islamic Azad University, Majlesi Branch, Esfahan, Iran

*Khanzade@gmail.com

(Manuscript Received --- 13 May 2024; Revised --- 02 July 2024; Accepted --- 21 July 2024)

Abstract

This study investigates the corrosion behavior and microstructural changes of Cu/Al/Cu three-layer tubes after post-weld heat treatment in the explosive welding process. The heat treatment was performed by varying the temperature. Polarization tests and electrochemical impedance spectroscopy were employed to examine the corrosion behavior of the weld zone. Additionally, metallographic examination using optical microscopy (OM) and scanning electron microscopy (SEM) was conducted to study the microstructure. The electrochemical impedance spectroscopy (EIS) results revealed that the "n" value in the heat-treated sample at 300°C and explosion load of 2.8 was lower than that of the heat-treated sample at 300°C and explosion load of 3.2. This indicates a higher corrosion current in the heat-treated sample at 300°C and explosion load of 2.8, resulting in a reduction in charge transfer resistance. In the comparison, we examined the effects of different temperatures and explosive load. Specifically, the heat-treated samples at 300°C temperature and 2.8 explosive load with variable annealing temperature and fixed annealing time were compared to those at 400°C temperature and 2.8 explosive load. The results demonstrated that the sample heat treated at 400°C exhibited a higher value of n (n=0.77) compared to the sample heat treated at 300°C with 2.8 explosive charge, which had a lower value of n (n=0.69). This difference in number n is attributed to the increase in the annealing temperature and the decrease in the energy stored in the interface.

Keywords: Explosive Welding, Explosive Load Thickness, Plastic Deformation, Vortex.

1- Introduction

Explosive Welding (EXW) is an exceptional solid-state welding technique that achieves bonding by propelling one component at an extremely high velocity using chemical explosives. Its primary application is the cladding of steel plates with a thin layer of corrosion-resistant material. However, there are inherent limitations regarding the producible geometries, typically limited to plates and tube sheets [1]. EXW is widely applicable to both similar and dissimilar materials, utilizing the force generated by detonation to create a metallic bond through electron sharing between the elements. Researchers have taken a keen interest in employing this welding technique in industries like shipbuilding, aircraft manufacturing, and aerospace, with a specific focus on sheet cladding and multilayer tank production [2]. Achieving high-quality EXW joints heavily relies on precise control of process variables, including surface preparation, joint clearance, detonation load quantity, explosion energy, and velocity [3-5]. Consequently, recent research endeavors have delved into various aspects of EXW, encompassing heat treatment of joints, permissible working temperatures, interface characteristics of the joint area, stand-off distance optimization, optimal explosive quantities, interlayer application, and their impact on energy loss [6-9]. The absence of heat in explosive welding distinguishes it from fusion welding techniques, eliminating many undesirable properties associated with heat-affected zones and thermal distortion [2, 3].

However, limited research has been conducted on the corrosion aspects of explosive welding. Acarer [10] studied the corrosion behavior of explosively bonded aluminum to copper, revealing galvanic

corrosion in the bond. The aluminum side exhibited a more anodic mode due to its higher electronegativity, resulting in a higher corrosion rate compared to the copper side. Mudali et al. [11] examined the corrosion of explosively bonded titanium and stainless steel 304. Their findings indicated that the bending stress in a nitric acid environment was within acceptable limits, and corrosion attacks were concentrated at the joint interface. Kengkla et al. [12] investigated the corrosion behavior of aluminum/steel explosive three-layer joints in military applications. They identified the formation of intermetallic compounds like Al_3Fe and Al_5Fe_2 at the joint interface, leading to a cathodic mode for aluminum and anodic mode for steel. As a result, preferential corrosion attacks were observed near the aluminum boundary and intermetallic compounds. Kahraman et al. [13] investigated the corrosion of explosively bonded titanium to stainless steel and found that the mass change of the bonded plates increased with an increase in explosive charge. This was attributed to plastic deformation and the formation of an oxide layer on the surface. They also examined the corrosion of Ti-6Al-4V and aluminum plates bonded through explosive welding [14]. Corrosion tests showed an initial high weight loss rate that decreased over time, with higher explosive charges leading to greater weight loss due to increased plastic deformation.

Furthermore, despite extensive research on explosive welding involving aluminum alloys and various metallic materials, the corrosion behavior of explosively welded Cu/Al/Cu joints and the effect of explosive welding heat treatment on it remains insufficiently explored. Previous studies have focused on aspects like the influence

of heat treatment on microstructure and mechanical properties of multilayer Cu/Al/Cu explosive welded joints by Gharah Shiran et al. [15], the role of flyer materials on the interface of Al/Cu explosive welds investigated by Carvalho et al. [16], and the effect of explosive ratio on bonding interface properties evaluated by Kaya [17]. However, the effect of explosive welding heat treatment on the corrosion behavior and microstructural changes in Copper-Aluminum-Copper Three-Layered Plates fabricated using the explosive welding technique, specifically considering different stand-off distances, have received inadequate attention. Hence, by addressing this overlooked aspect, this study aims to provide valuable insights into the effect of heat treatment on the corrosion behavior of explosively welded Cu/Al/Cu joints.

2- Experimental materials and methods

2-1- Materials

The alloys used in the explosive welding process to create the three-layer tube are Cu/Al/Cu, as shown in Tables 1 and 2 with their chemical compositions. The tubes are arranged in a completely parallel and concentric manner inside the containment vessel using an adjustable outlet system, either by exit or explosion outward. They are placed at specific gap distances relative to each other. The outer wall of the Cu tube is separated from the containment vessel by a suitable barrier material. Then, by introducing an appropriate explosive charge and aligning it with the inner wall of the alloy tube and the transition joint, the tube is accelerated towards its gap distance by the explosion, colliding with the Cu tube. Subsequently, the tube is accelerated towards its gap distance relative to the Cu tube, colliding

Table 1: Chemical Composition of Al Series 1000 (wt%)

Al	Cr	Cu	Fe	Mg	Mn	Si	Zn
Bal.	0.1	0.2	0.72	0.9	0.028	0.23	0.21

Table 2: Chemical Composition of Cu (wt%)

Cu	Sn	Pb	P	Zn
Bal.	0.92	0.0123	0.0892	0.119

with it, resulting in simultaneous joining, and a two-layer tube is formed.

In the welding process, a 2 mm stand-off distance was used, and the tubes were arranged in a fully parallel and concentric manner relative to each other at the specified stand-off distances. The welding operation was performed. For tube joining, an explosive material called Amatol, which is a combination of trinitrotoluene or TNT and ammonium nitrate, was used.

Alloy tube made of Cu and Al is considered as a flying tube in explosive welding. It has a thickness of 1.5 mm and a length of 240 mm. This tube is designed and used to bond to the base tube for bonding at various diameters to create suitable stand-off distances.

Table 3 represents the dimensions of the tubes. The tube is considered as the base tube and is made of copper, with a thickness of 4.5 mm and a length of 200 mm. The dimensions of the tube remain constant throughout the bonding process, with an outer diameter of 135 mm and an inner diameter of 126 mm. To prevent the base tube's outer surface from bonding with the containment vessel and facilitate easy separation of the welded assembly, a suitable filling material such as rubber with a thickness of approximately 5 mm is used. This filling material is carefully placed

between the outer surface of the base tube and the containment vessel prior to the explosive welding operation. Fig. 1 illustrates a set-up of tubes and explosive welding equipment.

Due to the investigation of the effects of explosive load, temperature, and time of heat treatment on the intermetallic compounds (IMCs), samples of spaced tubes with different stand-off distances were prepared. The samples underwent post-welding heat treatment. Heat treatment was conducted in a furnace with the following parameters: argon protection, pressure of 100 kPa, temperatures of 300 and 400°C, and

durations of half an hour. Afterward, the samples were cooled to room temperature (Table 4).

2-2- Structural and Metallurgical Examination Tests (Methodology)

In order to conduct structural studies, the samples underwent a step-by-step preparation process. Initially, the samples were sanded with SiC ranging from No. 60 to 2500, ensuring a gradual refinement of the surface. Subsequently, the samples were polished using a diamond-like paste and/or an Al_2O_3 solution.

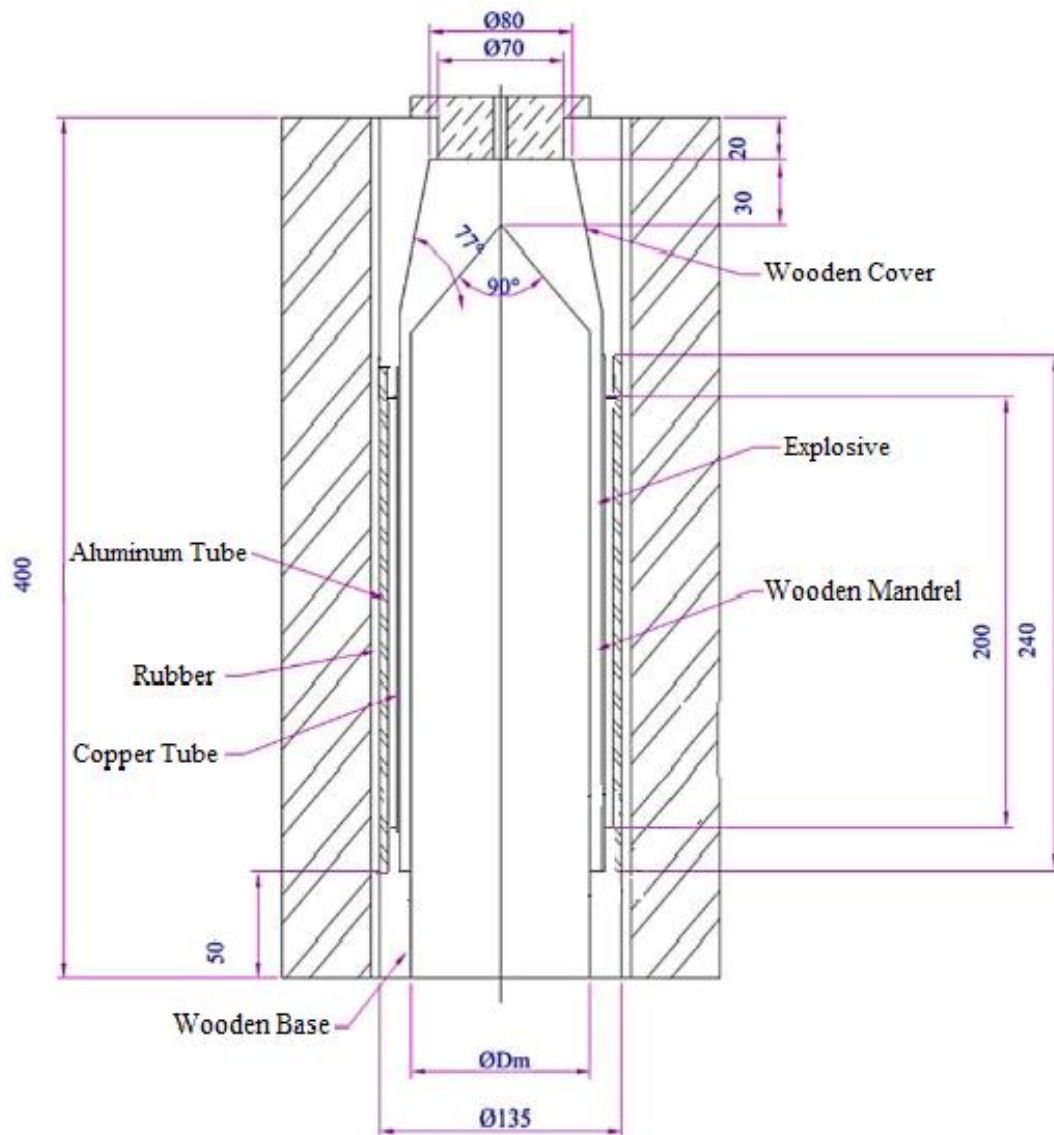


Fig. 1 Set-up of tubes and explosive welding equipment.

Length (mm)	Thickness (mm)	I. D. (mm)	O. D. (mm)	Material
240	1.5	118	121	Cu
240	1.5	49.5, 96	104.5, 106	Al
200	4.5	126	135	Cu

Table 4: Sample designation based on gap distance, temperature, and duration of heat treatment

Sample	explosive load	Time (min)	Tem. (°C)	Standoff distance (mm)	Atmo.
1	2.8	30	300	3	Air
2	2.8	30	400	3	Air
3	3.8	30	300	3	Air
4	3.8	30	400	3	Air

The polished samples were then examined under different magnifications using an optical microscope (OM), scanning electron microscope (SEM), and Energy Dispersive X-ray Spectrometry analysis (EDS) to observe the interface area and the IMCs formed within it. After the polishing process, the surface of the samples was thoroughly washed with alcohol and dried. Next, the samples underwent chemical etching using a solution composed of glycerin, nitric acid, and chloride acid. This etching process allowed for the visualization and analysis of the IMC layer's thickness. The shape of the interface and IMCs was analyzed using an OM, specifically the Metallux 3 model. By following this preparation and examination

procedure, comprehensive insights into the structure, interfacial characteristics, and IMC formation were obtained,

facilitating a better understanding of the sample's properties.

To study the corrosion behavior of explosively welded components in a 3.5% NaCl solution, a three-electrode electrochemical cell was used. The cell had a capacity of 500 ml and consisted of a saturated calomel electrode (SCE) as the reference electrode, a platinum electrode as the auxiliary electrode, and the samples as the working electrode. Potentiodynamic polarization experiments were performed with a scan rate of 1 mV/s, ranging from 250 mV below the open circuit potential to 250 mV above it. These tests were conducted according to ASTM G59-97 to determine the corrosion potential and corrosion current. Additionally, electrochemical impedance spectroscopy (EIS) tests were conducted in a frequency range of 100 kHz to 10 mHz with a 10 mV amplitude around the open circuit potential. The duration of the EIS tests was set at 90 minutes, following ASTM G106 guidelines.

3- Results and Discussion

3-1- Examination of the Microstructure of the Samples Using OM

As observed in Fig. 2(a), the joint interface in sample with 2.8 explosive load before heat treatment appears to be flat. During the explosive welding process, due to the high intensity of forces and very short duration, a single-layer joint is formed between the two metals at the joint interface, which undergoes severe deformation. Additionally, Fig. 2(a) shows the presence of new phases in limited areas of the joint interface. This intermediate phase is a characteristic feature of explosive welding and is formed due to localized melting zone at the joint interface. Due to the stand-off

distance between the flyer tube and the interlayer (2.8 mm), the impact speed is low, and the plastic deformation caused by the impact and as a result, the bonding interface before heat treatment is flat. The images obtained from OM in Figs. 2(b) and 2(c) for samples with 2.8 explosive load after heat treatment demonstrate the formation and growth of IMCs at the joint

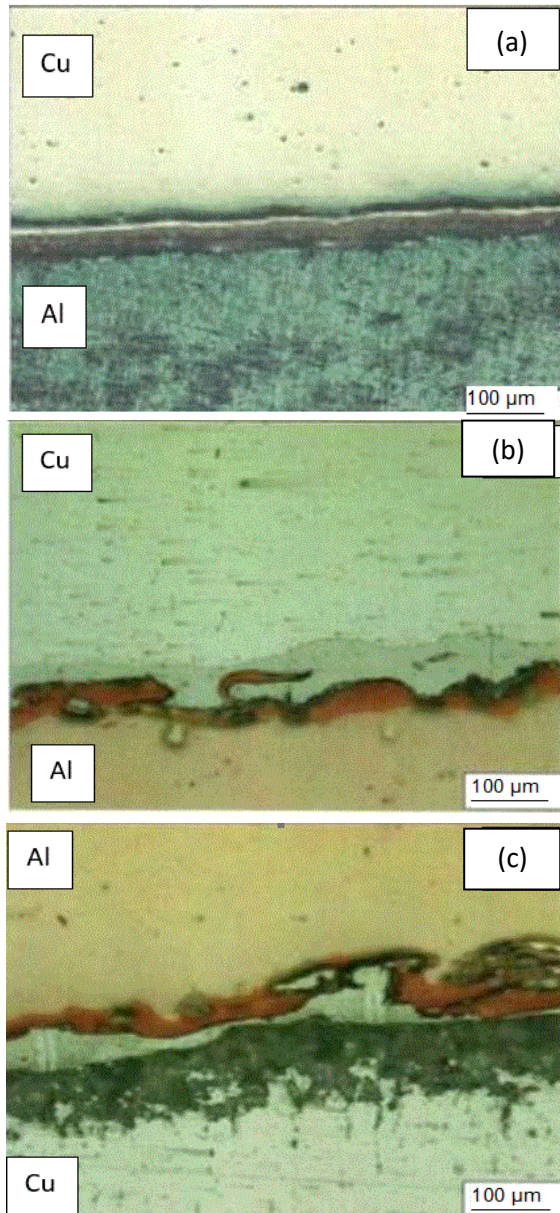


Fig. 2 Joint interface of Sample with 2.8 explosive load: a) Untreated, b) Heat-treated at 300°C for 30 min, c) Heat-treated at 400°C for 30 min

interface with increasing temperature during the heat treatment process. The images obtained from OM in Figs. 2(a) and 2(c) indicate the formation and growth of IMCs at the joint interface with increasing temperature during the heat treatment process. The rise in temperature during heat treatment activates the diffusion mechanism and leads to the formation of IMCs at the joint interface.

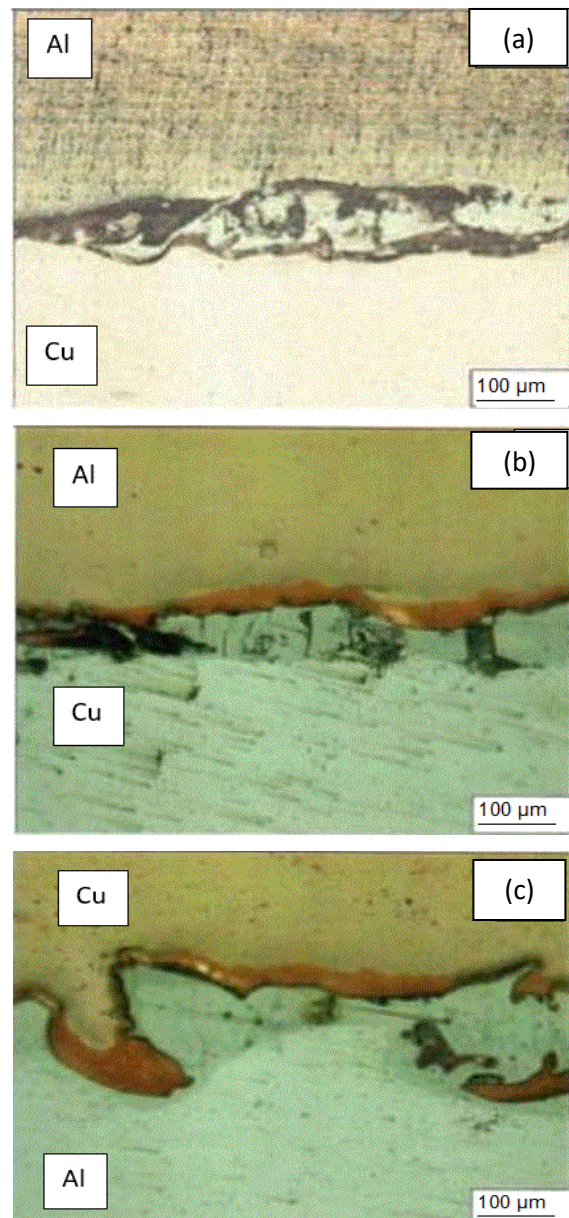


Fig. 3 Joint interface of Sample with 3.8 explosive load: a) Untreated, b) Heat-treated at 300°C for 30 min, c) Heat-treated at 400°C for 30 min

Considering the formation of IMCs during explosive welding, as shown in Fig. 2(a), these compounds facilitate the easier diffusion of Al and Cu atoms during the heat treatment process. The findings from the aforementioned studies are in line with the observations reported by Carvalho et al. [16] and Loureiro et al. [18].

The microstructure of the sample with 3.8 explosive load is observed in Fig. 3, where the OM images depict the Al/Cu joint before and after the heat treatment process. The joint interface exhibits a short wave-like geometry, and the heat treatment process has no significant impact on the wave-like pattern. In comparison to other joint geometries, the waveform joint is preferred for explosive weld joints due to its larger contact surface area and higher strength [19]. By comparing samples with 2.8 and 3.8 explosive load, it can be concluded that an increase in the explosive load from 2.8 to 3.8 leads to the transformation of a flat joint interface into a wave pattern. Considering the significant density difference between Al and Cu, a thin molten layer is formed, as shown in Fig. 3(a), which leads to the creation of various compounds at the joint interface. The reason behind this is the generation of localized heat and shear stress at a high rate at the joint interface. The heat-treated samples can be observed in Figs. 3(b) and 3(c), respectively. Studies conducted by Samardzic [20], and Banker [21] also demonstrated that the width of IMCs increases with the temperature of the heat treatment process in Al/Cu explosive welding joints. By comparing the samples in Figs. 2 and 3, it can be observed that with an increase in the temperature of the heat treatment process, the thickness of

the localized molten layer gradually increases.

3-2 Microstructural Examination by SEM

Fig. 4 illustrates the SEM images of the joint interface of sample with 2.8 explosive load and the thickness of layers at certain points. As shown in the provided images, a flat joint interface is formed in this test. As evident from the OM, SEM, and Fig. 4(a) for the pre-heat-treated sample, the thickness of these layers is higher compared to after performing heat treatment at temperatures of 300°C and 400°C for 30 min, as shown in Figs. 4(b) and 4(c). The reason behind this is the effect of the heat treatment process and the diffusion of alloying elements, which also resulted in the expansion of IMCs. Shiran et al. [15] and Samardzic et al. [20] have also obtained similar findings when studying the effect of heat treatment on the explosive welding properties of Cu/Al/Cu and Almg-Al-Steel, respectively.

Results of EDS analysis of the scanning electron microscope (Fig. 4), showing the presence of compounds in the joint interface. According to Fig. 4, the obtained results before the heat treatment process showed that the alloying structure compounds consist of 11.71 at.% Al and 88.60 at.% Cu.

The results indicate the formation of IMCs in localized melting areas of the alloy. For non-homogeneous compounds, based on the reflection of the jet from the lower-density tube, pressure is mainly exerted on the higher-density tube, resulting in a vortex formed behind the shockwave containing interfacial tube materials, and a vortex formed in front of the waves containing base tube materials. Furthermore, the results show that the

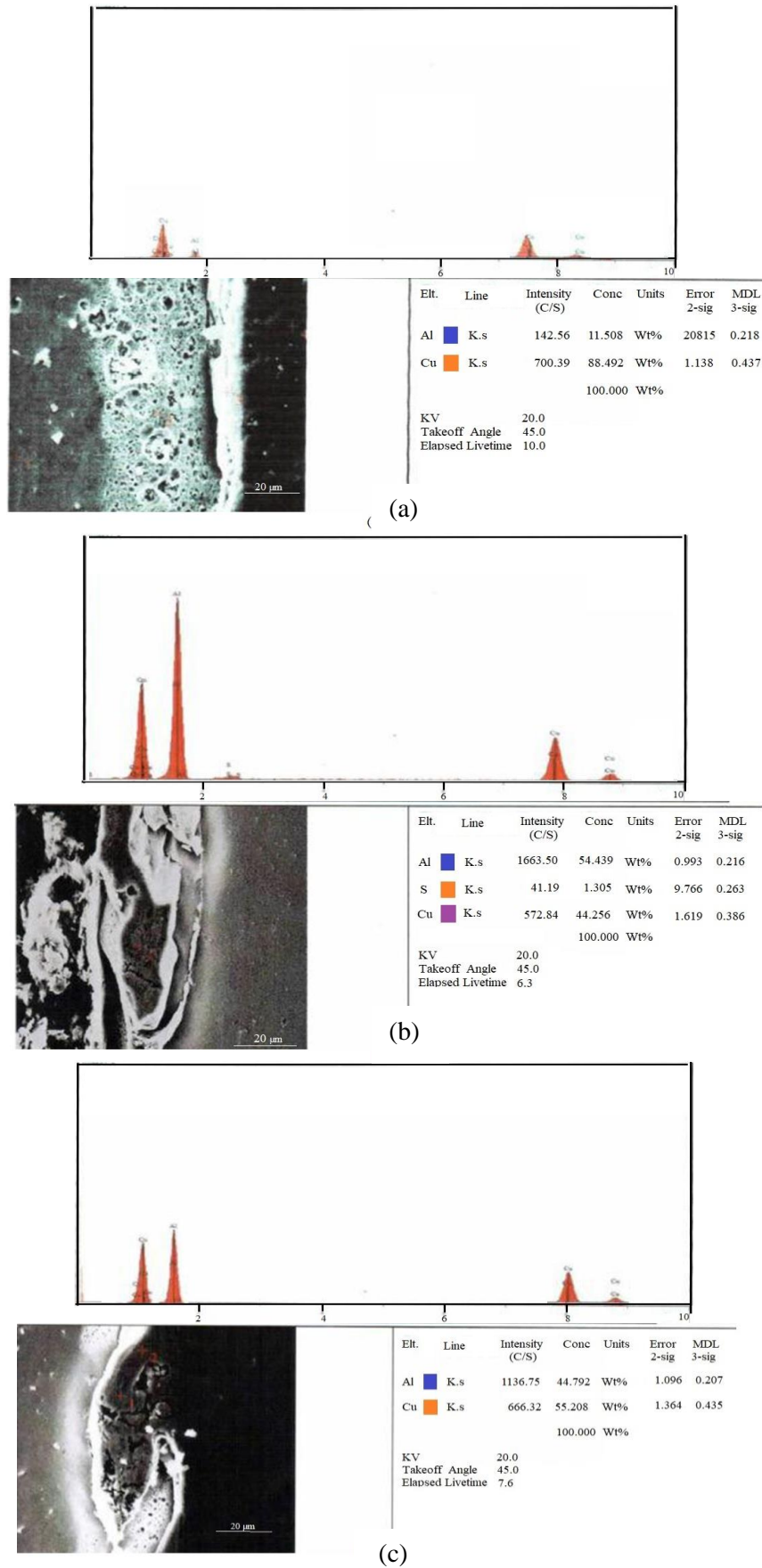


Fig. 4 Joint interface of Sample 1: a) Untreated, b) Heat-treated at 300°C for 30 min, c) Heat-treated at 400°C for 30 min

analysis of these compounds changes in the vicinity of different waves with variations in welding parameters and becomes non-uniform, as observed in Fig. 4(a). It is evident that compared to the observed changes in the percentage of Al and Cu elements, in the samples before and after the heat treatment process, conditions are created for the diffusion of elements and the formation of IMCs with an increase in temperature [21, 22].

Fig. 5 illustrates the microstructure of the joint interface and the intermetallic layer between the metals in sample with 3.8 explosive load before and after heat treatment. Although explosive welding is a solid-state process, localized melting zones can be observed near the joint interface, as shown in Fig. 5(a). Due to the high collision pressures, the formation of a vortex at the interface can occur, leading to localized melting zones in certain areas. These zones are a result of internal heating caused by the intense pressure of explosive shockwaves, significant plastic deformation, and heat generation from the collapse of vortices ahead of certain wavefronts. This heat is generated through the conversion of kinetic energy into thermal energy during collisions. Additionally, adiabatic heating occurs due to confined gases between the tubes. These areas are surrounded by colder metal and experience a rapid cooling rate ranging from 10^5 to 10^7 K / S [19].

In Fig. 5(b), the atomic percentage of Al to Cu is 50.03 and 44.53, respectively. The intermetallic layer shown in Fig. 5(c) exhibits atomic percentages of Al to Cu as 39.36 and 56.36, respectively.

The images obtained from the SEM indicate the formation and growth of IMCs in the joint interface of Al/Cu with increasing temperature during the

annealing heat treatment process. Carvalho et al. [3], Jiang et al. [8] and Shiran et al. [15] reported that the temperature increase activates the diffusion mechanism and formation of IMCs in the joint interface of the connection. If IMCs are formed during explosive welding, it facilitates easier diffusion of Al and Cu atoms during the heat treatment of the samples [15, 24].

However, based on the obtained EDS analysis, the IMC layer in samples 1-4 probably contains Al_3Cu , Al_2Cu IMCs. These results are in accordance with the study conducted on multilayer Cu/Al/Cu explosive welded joints [15].

3-3- Results of Potentiodynamic polarization

Fig. 6 illustrates the polarization curves of the explosively welded samples after the heat treatment process. Electrochemical parameters extracted from these curves, such as corrosion potential (E_{corr}), corrosion current density (I_{corr}) (corrosion rate), and Tafel slopes for the anodic and cathodic reactions obtained through Tafel extrapolation, are reported in Table 5.

In general, the parallelism of the cathodic Tafel branches in Fig. 6 indicates that the hydrogen evolution is under activation control, and the mechanism of H^+ ion reduction on the sample surfaces is not significantly influenced by the joining process. The results in Table 5 show that with an increase in annealing temperature, the corrosion potential shifts towards positive values, and the corrosion current density decreases from 175.39 to 19.64 $\mu A/cm^2$. Shiran et al. [25] and Peykari et al. [26] reported that the reason for this reduction is the decrease in the energy of the joint interface resulting from the

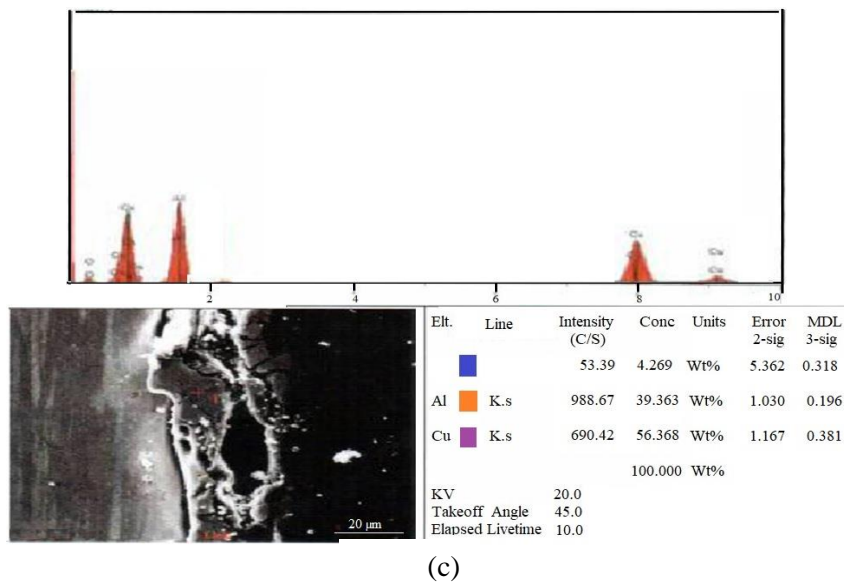
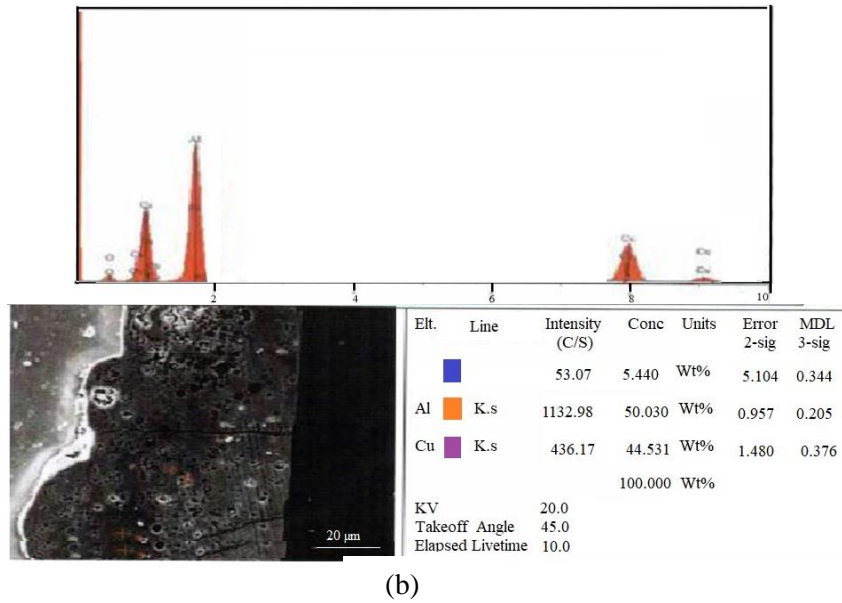
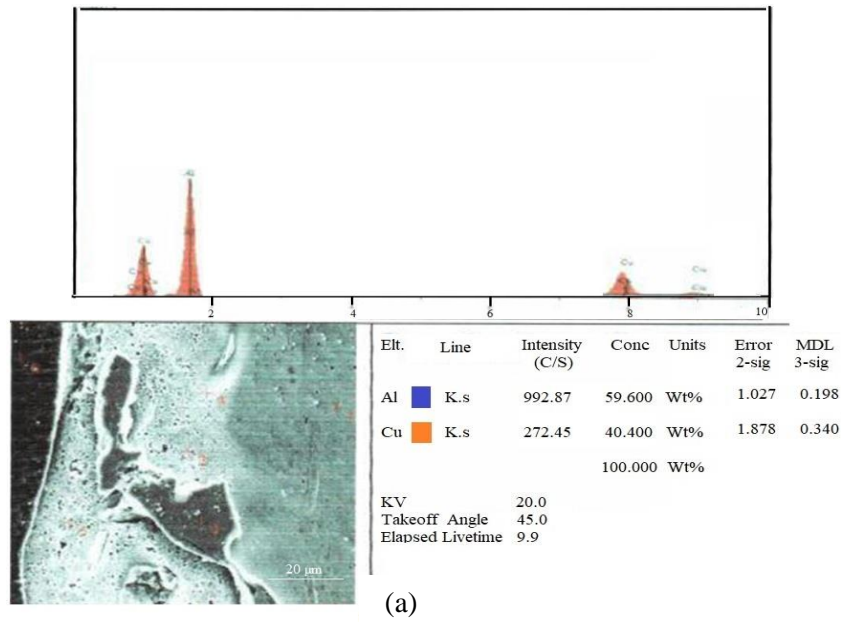


Fig. 5 Joint interface of Sample with 3.8 explosive load: a) Untreated, b) Heat-treated at 300°C for 30 min, c) Heat-treated at 400°C for 30 min

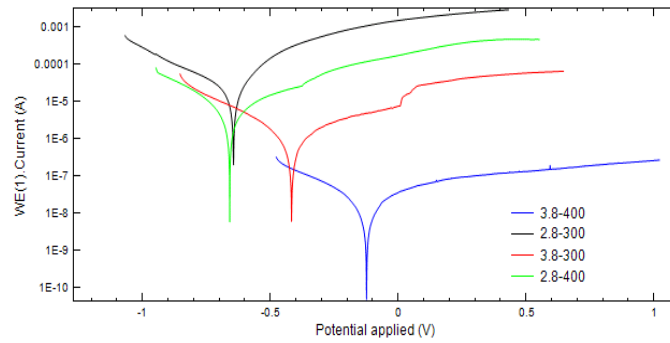


Fig. 6 Potentiodynamic Polarization Curves of the explosively welded samples after the heat treatment process

Table 5: Electrochemical Parameters obtained from the Potentiodynamic Polarization Curves of the explosively welded samples after the heat treatment process in a 3.5% NaCl solution at room temperature

Sample	Temperature (°C)	Time (min)	i_{corr} ($\mu\text{A cm}^{-2}$)	E_{corr} (mV)	β_a (mV dec^{-1})	β_c (mV dec^{-1})	Explosive load
1	300	30	175.39	-677	134	271	2.8
2	400	30	126.80	-690	150	237	2.8
3	300	30	62.61	-436	135	288	3.8
4	400	30	19.64	-116	142	268	3.8

release of stored energy, which leads to a decrease in corrosion.

Moreover, based on the elemental analysis, it can be concluded that with an increase in annealing temperature, the Cu content in the molten layer increases, which contributes to the improvement of this layer.

3-4 Analysis of Electrochemical Impedance Spectroscopy Results

The Nyquist plots corresponding to the explosively welded samples after the heat treatment process are shown in Fig. 7. The EIS data were obtained and fitted using the equivalent circuit presented in Fig. 8, which exhibited good agreement with the experimental results and are observed in Table 6.

From Fig. 7, it is evident that the impedance loops obtained in the Nyquist plot exhibit slight deviation from a perfect semicircle, which is known as the depressed semicircle effect.

Generally, the deviation from a perfect semicircle is attributed to frequency dispersion, surface heterogeneity, and mass transfer resistance. This difference is described by the behavior of the non-ideal double layer as a capacitor. Therefore, the use of a Constant Phase Element (CPE) instead of the non-ideal capacitive behavior of the double layer is necessary to account for the relaxation times distribution arising from non-uniformities on micro or nano surfaces, such as roughness, porous layer, impurities, inhibitor adsorption, penetration, etc., in order to achieve more accurate matching

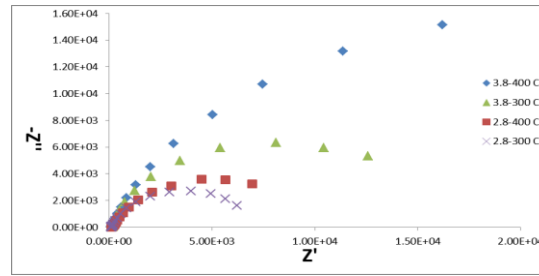


Fig. 7 Nyquist plots of the explosively welded samples after the heat treatment process

Table 6: EIS Data obtained from the explosively welded samples after the heat treatment process in a 3.5% NaCl solution at room temperature

Sample	Temperature (°c)	Time (min)	R_s (Ω)	R_p ($\Omega \text{ cm}^{-2}$)	C_{dl} ($\mu\text{F cm}^{-2}$)	n	explosive load
1	300	30	8.53	7601	310	0.69	2.8
2	400	30	3.59	14260	200	0.77	2.8
3	300	30	4.93	17140	420	0.80	3.8
4	400	30	7.09	38450	450	0.82	3.8

of results. The impedance of a CPE is expressed by the following equation:

$$Z_{\text{CPE}} = [Y_0(j\omega)^n]^{-1} \quad (1)$$

In this equation, Y_0 represents the relative admittance factor, and n is the non-ideality coefficient of the surface (phase shift). A larger value of n indicates greater continuity and uniformity in the joint interface. In this case, the corrosion current is lower because the corrosion current is proportional to the contact area between the solution and the metal. As defects and discontinuities increase, the effective contact area between the solution and the metal increases, resulting in an increase in the corrosion current. For the CPE, values of $n=0, 1,$ and -1 correspond

to purely resistive, purely capacitive, and purely inductive behaviors, respectively [26].

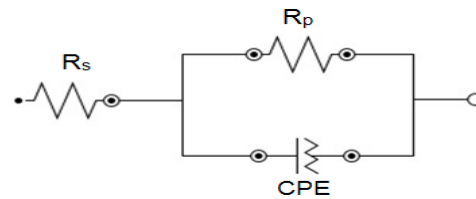


Fig. 8 Equivalent electrical circuit diagram used for modeling the behavior of the metal-solution joint interface

In this study, the diameter of the Nyquist plots in Fig. 7, which is considered as the polarization resistance (R_p), represents the only existing capacitive loops associated with the charge transfer resistance between the metal and the outer Helmholtz layer (OHP). These observations indicate that the corrosion of

the metal is controlled by a charge transfer process.

The double electric layer can be well described by using an equivalent circuit and presenting a suitable model for the metal/solution interface. The corresponding equivalent electrical circuit for the samples in the solution is shown in Fig. 9(a), providing a schematic model of the potential distributions in the metal/solution interface (Fig. 9(b)) and the resistances associated with the double layer (Fig. 9(c)). In the presence of inhibitors, the polarization resistance (R_p) includes the charge transfer resistance (R_{ct}), the inhibitor layer resistance on the metal surface (R_f), the accumulated particles (inhibitor molecules, corrosion products, etc.) in the metal/solution interface (R_a), and the diffusion layer resistance (R_d) ($R_p = R_{ct} + R_f + R_a + R_d$) [26].

The double layer capacitance (C_{dl}) is calculated using the following equation:

$$f(-Z''_{max}) = \frac{1}{2\pi C_{dl} R_{ct}} \quad (2)$$

In this equation, $-Z''_{max}$ represents the maximum value of the imaginary component of the impedance. According to Table 6, the value of “n” in the sample subjected to heat treatment at a temperature of 300°C and an explosive load of 2.8 is lower than the sample subjected to heat treatment at a temperature of 300°C and an explosive load of 3.8. Therefore, the corrosion current in the sample subjected to heat treatment at 300°C and an explosive load of 2.8 is higher, resulting in a decrease in the charge transfer resistance. By comparing the samples subjected to heat treatment at 300°C and an explosive load of 2.8 and the samples subjected to heat

treatment at 400°C and an explosive load of 2.8, with variable annealing temperatures and constant annealing time, it is observed that the sample heat-treated at 400°C has a higher value of “n” ($n=0.77$) compared to the sample heat-treated at lower annealing temperature, 300°C ($n=0.69$), and the reason for this is the increase in annealing temperature and the decrease in stored energy in the metal/solution interface. Based on the results obtained from the atomic percentage of localized melting layers and electrochemical test results, it can be inferred that with increasing temperature during the heat treatment process, the corrosion resistance decreases due to an increase in copper concentration (improvement of the localized melting layer).

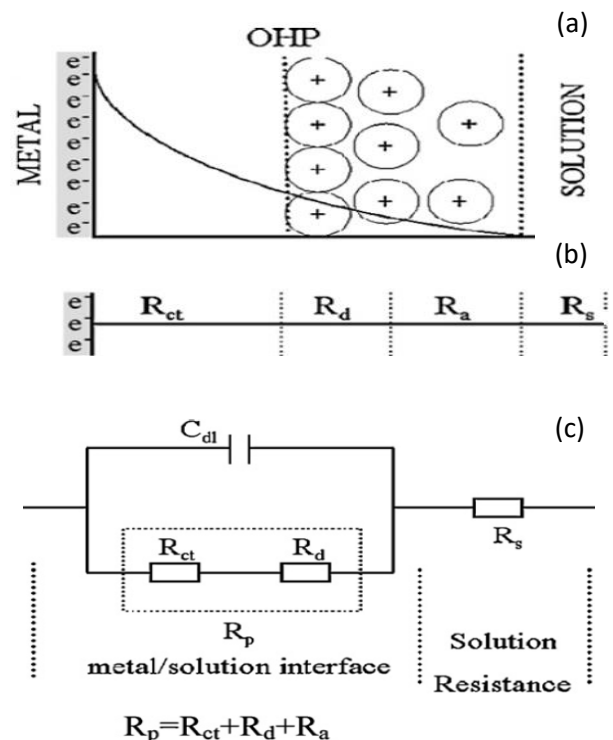


Fig. 9 Potential distributions at (a) metal/solution interface, (b) resistances corresponding to dual layer and (c) proposal electrical equivalent circuit for non-preventing solution [26]

4- Conclusion

In this study, the corrosion behavior and microstructural changes of explosively welded three-layered Cu/Al/Cu tubes were investigated, and the following results were obtained:

1. Based on the results obtained from OM, the thickness of the localized melting layer gradually increases with an increase in the temperature of the heat treatment process. The atomic percentage of Al decreases gradually, while the atomic percentage of Cu increases. With an increase in the explosive load from 2.8 to 3.8, the morphology of the joint interface changes from flat to wavy.
2. SEM images indicate the formation and growth of IMCs at the Al/Cu joint interface with an increase in the temperature of the heat treatment process. The temperature increase activates the diffusion mechanism and the formation of IMCs at the joint interface.
3. With an increase in temperature and time during the heat treatment process, the corrosion resistance decreases due to a decrease in stored energy and an increase in Cu concentration at the joint interface, leading to a gradual reduction in the galvanic corrosion potential.
4. The electrochemical impedance spectroscopy results indicate that the value of “n” in the sample subjected to heat treatment at 300°C and an explosive load of 2.8 is lower than that of the sample subjected to heat treatment at 300°C and an explosive load of 3.8. Consequently, the corrosion current in the sample treated at 300°C and an explosive load of 2.8 is higher, leading to a decrease in charge transfer resistance. Based on the results obtained from the atomic percentage of localized melting layers and electrochemical test results, it can be

inferred that with an increase in the temperature of the heat treatment process, the corrosion resistance decreases due to an increase in Cu concentration (resulting in an improvement of the localized melting layer).

References

- [1] Chen, X., Xie, X., Hu, J., Li, X., Luo, N., Huang, J. & Liang, G. (2024) Experimental and numerical study on the mechanism of interlayer explosive welding. *Journal of Materials Research and Technology*, 30, 5529–5546.
- [2] Sherpa, B.B., Yu, M., Inao, D., Tanaka, S. & Hokamoto, K., (2024) Explosive welding of aluminum and cast iron for potential transportation and structural applications. *Advanced Engineering Materials*, 26, 2301389–2301399.
- [3] Carvalho, G.H.S.F.L., Galvão, I., Mendes, R. & et al. (2019) Weldability of aluminium-copper in explosive welding. *International Journal of Advanced Manufacturing Technology*, 103, 3211–3221.
- [4] Liu, B.X., Yin, F.X., Dai, X.L., He, J.N., Fang, W. & Chen, C.X., (2017) The tensile behaviors and fracture characteristics of stainless steel clad plates with different interfacial status. *Materials Science and Engineering A*, 679, 172–82.
- [5] Acarer, M. & Demir, B. (2008) An investigation of mechanical and metallurgical properties of explosive welded aluminum–dual phase steel. *Materials Letters*, 62, 4158–60.
- [6] Zhang, T., Wang, W., Zhang, W., Wei, Y., Cao, X. & Yan, Z. (2018) Microstructure evolution and mechanical properties of an AA6061/AZ31b alloy plate fabricated by explosive welding. *Journal of Alloys and Compounds*, 735, 1759–68.
- [7] Bataev, I.A., Lazurenko, D.V., Tanaka S., Hokamoto, K, Bataev, A.A. & Guo, Y. (2017) High cooling rates and metastable phases at the interfaces of explosively welded materials. *Acta Materialia*, 135, 277–89.
- [8] Jiang, L., Luo, N., Liang, H. & Zhao, Y. (2022) Microstructure and texture distribution in the bonding interface of Cu/Al composite tube fabricated by explosive welding. *The*

- International Journal of Advanced Manufacturing Technology*, 123, 3021-3031.
- [9] Aceves, S.M., Espinosa-Loza, F., Elmer, J.W. & Huber, R. (2015) Comparison of Cu, Ti and Ta interlayer explosively fabricated aluminum to stainless steel transition joints for cryogenic pressurized hydrogen storage. *International Journal of Hydrogen Energy*, 40, 1490–503.
- [10] Acarer, M., (2012) Electrical corrosion, and mechanical properties of aluminum- copper joints produced by explosive welding. *Journal of Materials Engineering and Performance*, 21, 2375–9.
- [11] Kamachi Mudali, U., Ananda Rao, B.M., Shanmugam, K., Natarajan, R. & Baldev R. (2003) Corrosion and microstructural aspects of dissimilar joints of titanium and type 304L stainless steel. *Journal of Nuclear Materials*, 321, 40-48.
- [12] Kengkla, N. & Tareelap, N. (2012) Role of intermetallic compound on corrosion of aluminium/steel transition joint used in naval applications. *Proc. of the 1st Mae Fah Luang University Int. Conf. (MFUIC2012) (Chiangrai Thailand)*.
- [13] Kahramana, N., Gülenç, B. & Findik, F. (2005) Joining of titanium/stainless steel by explosive welding and effect on interface. *Journal of Materials Processing Technology*, 169, 127–33.
- [14] Kahramana, N., Gülenç, B. & Findik, F. (2007) Corrosion and mechanical/microstructural aspects of dissimilar joints of Ti–6Al–4V and al plates. *International Journal of Impact Engineering*, 34, 1423–32.
- [15] Shiran, M.K.G., Khalaj, G., Pouraliakbar, H., Jandaghi, M.R., Dehnavi, A.S. & Bakhtiari, H. (2018) Multilayer Cu/Al/Cu explosive welded joints: characterizing heat treatment effect on the interface microstructure and mechanical properties. *Journal of Manufacturing Processes*, 35, 657–663.
- [16] Carvalho, G.H.S.F.L., Mendes, R., Leal, R.M., Galvão, I. & Loureiro, A. (2017) Effect of the flyer material on the interface phenomena in aluminium and copper explosive welds. *Materials and Design*, 122, 172–183.
- [17] Kaya, Y. (2018) Investigation of copper-aluminium composite materials produced by explosive welding. *Metals*, 8, 780-791.
- [18] Loureiro, A., Mendes, R. & Ribeiro, J.B. et al. (2016) Effect of explosive mixture on quality of explosive welds of copper to aluminum. *Materials Design*, 95, 256-267.
- [19] Sherpa, B.B., & Rani, R. (2024) Advancements in explosive welding process for bimetallic material joining: A review. *Journal of Alloys and Metallurgical Systems*, 6, 100078-100092.
- [20] Samardzic, I., Matesa, B. & Kladaric, I. (2011) The influence of heat treatment on properties of three-metal explosion joint: Almg-Al-Steel. *Metabk*, 50, 159-162.
- [21] Banker, J. (2002) Aluminum-steel electric transition joints, effects of temperature and time upon mechanical properties. *Draft of Paper for presentation TMS 131st Annual Meeting*.
- [22] Meyers, M.A., Xu, Y.B. & Xue, Q. (2003) Micro structural evolution in adiabatic shear localization in stainless steel. *Acta Materialia*, 51, 1307–1325.
- [23] Murr, L.E., Ferreyra, E, Pap, E., Rivas, J.M., Kennedy, C., Ayapu, A, Garcia, E.I., Sanchez, J.C., Huang, W. & Niou, C. S. (1996) Novel deformation processes and microstructures involving ballistic penetrator formation and hypervelocity impact and penetration phenomena. *Materials Characterization*, 37, 245-276.
- [24] Bakhtiari, H., Abbasi, H., Sabet, H., Khanzadeh, M.R. & Farvizi, M. (2022) Investigation on the effects of explosive welding parameters on the mechanical properties and electrical conductivity of Al-Cu bimetal. *Journal of Environmental Friendly Materials*, 6, 31-37.
- [25] Shiran, M.R.K.G., Razazi, M., Bakhtiari, H. & Tavira, A. (2018) Evaluation of welding parameter's effects on corrosion behavior of bronze-carbon steel dual-layer explosion welded joint at salt environment. *Materials Research*, 21, 1-7.
- [26] Peykari, R., Khanzadeh, M.R. & Bakhtiari, H. (2022) The Effect of explosive welding variables on corrosion behavior of 304 stainless steel-copper joint in 3.5% NaCl solution concentration environment. *Journal of Simulation and Analysis of Novel Technologies in Mechanical Engineering*, 14, 0025~0036.